J Solution Chem (2015) 44:293–306
DOI 10.1007/s10953-015-0304-6

Spectroscopic Investigation of the Interaction of Pyridinium Surfactant with Bovine Serum Albumin

Zijia Liu · Xiangfeng Guo · Zhuo Feng · Lihua Jia

Received: 2 October 2013 / Accepted: 25 November 2014 / Published online: 14 February 2015

Abstract The interaction of 1-dodecyl carbamoyl methylene pyridinium chloride (DAPC) with bovine serum albumin (BSA) was investigated by UV–Vis absorption, CD and fluorescence spectroscopies. The results of fluorescence titration reveal that DAPC strongly quenched the intrinsic fluorescence of BSA and caused a blue shift of the emission wavelength through a static quenching mechanism. The reduction of the binding constant (K_A) and number of binding sites (n) between DAPC and BSA was studied with increasing temperature. The binding process is exothermic and entropy driven. The distance r between the donor of BSA and the acceptor of DAPC decreases with increasing concentration of DAPC. Furthermore, CD spectra and synchronous fluorescence spectra shows that DAPC induced conformational changes of BSA.

Keywords Bovine serum albumin · Pyridinium cationic surfactant · Spectroscopy · Interaction

1 Introduction

Proteins play a vital role in life process, and they can bind a wide range of ligands, including metal ions, surfactants, drugs and so on [1–5]. In recent years, attention has been focused mainly on the interactions between surfactants and proteins, not only because of their application to the food, medicine, cosmetic, biological and other fields, but also as models of biological system, to accelerate biological technology for the chemical industry, medicine and other traditional fields [6–10]. Among various

Z. Liu · X. Guo (✉) · Z. Feng · L. Jia (✉)
Key Laboratory of Fine Chemicals of College of Heilongjiang Province, College of Chemistry and Chemical Engineering, Qiqihar University, Qiqihar 161006, People's Republic of China
e-mail: xfguo@163.com

L. Jia
e-mail: jlh29@163.com

bio-macromolecules, serum albumin is the most abundant soluble protein in the circulatory system of a wide variety of organisms, and possesses many physiological functions. The most outstanding function of serum albumins is that they serve as a depot protein and transport protein for many compounds [11, 12]. Bovine serum albumin (BSA) is the protein commonly used for research purposes, due to its stability, solubility and versatile binding ability and especially its structural homology with human serum albumin (HSA) [13].

Most of studies about the interaction of protein–surfactant have concentrated mainly on common surfactants such as cetyltrimethyl ammonium bromide (CTAB) [14], sodium dodecylsulfate (SDS) [15], tert-octylphenoxy polyethoxyethanol (X-100) [16], cationic cethyltrimethylammonium (CTAC) [17], polyoxyethylene(20) sorbitan monolaurate (Tween-20) and so on [18]. In the recent years, pyridinium cationic surfactants with antibacterial properties have been developed with countless applications in various areas such as germicides and fungicides, cosmetic products, pharmaceutical preparations, household products, gene delivery agents, corrosion inhibitors and so on [19]. Usually, pyridinium cationic surfactants possess direct anti-inflammatory activity and inhibiting action on several matrix metalloproteinase proteins, which cause inflammation, and they are used as disinfectants for eating and drinking utensils and food processing equipment. Moreover, their antimicrobial activity is also employed in the dairy industry for sanitization of milk cans and milking machines [20]. Pyridinium cationic surfactants are considered to be non-toxic when adsorbed on the skin, but can be highly toxic if ingested [21]. If they enter the bloodstream, they would interact with serum albumin [22]. Therefore, the interaction of pyridinium cationic surfactants with serum albumin is interesting for human health and life quality.

In the present work, the interaction of BSA with 1-dodecyl carbamoyl methyl pyridinium chloride (DAPC) was probed by means of steady-state fluorescence, UV–Vis and CD spectrophotometries. The binding constant, number of binding sites and standard state thermodynamic parameters were calculated. The binding forces, energy transfer and conformation are also discussed. This study investigates the binding affinity and binding mechanism at the molecular level and it may offer a better understanding for the bactericidal efficiency of pyridinium surfactants (Scheme 1).

2 Materials and Methods

2.1 Apparatus

Fluorescence measurements were conducted on an F-4500 fluorescence spectrophotometer (Hitachi, Japan) equipped with a thermostat bath and 1.0 cm quartz cells; the slit widths were set at 5 and 10 nm. The UV spectrum were measured using a TU-1901 UV–Vis spectrophotometer (Persee, China) equipped with 1.0 cm quartz cells. The CD spectra were recorded on a MOS-450 spectropolarimeter (France, Bio-Logic) equipped with 0.10 cm quartz cells.

Scheme 1 Structure of DAPC

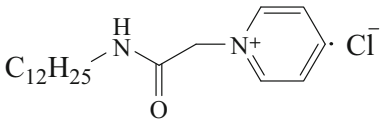

2.2 Reagents

BSA was purchased from Beijing Boxing Biological Company and was dissolved in Tris–HCl buffer solution with pH = 7.40 containing 0.02 mol·L^{-1}·NaCl, and stored at 0–4 °C. The BSA concentration was fixed at 1.0 μmol·L^{-1}; DAPC was synthesized and purified according to the reported literature [19] and the DAPC (5.0 μmol·L^{-1}) solution was prepared in Tris–HCl buffer solution (0.02 mol·L^{-1}, pH = 7.40, 0.02 mol·L^{-1} NaCl). All the reagents were analytical reagent. All of the solutions were prepared using ultrapure water.

2.3 Procedures

A 5.0 μmol·L^{-1} solution of DAPC was added gradually to 20 mL of the solution of BSA (1.0 μmol·L^{-1}) using a microinjector with final concentrations of DAPC ranging from 0 to 3.0 μmol·L^{-1}. 3.0 mL of solution was used to fill a quartz cell with an optical path length of 1 cm. The fluorescence spectra were recorded at different temperatures of 298, 308 and 318 K, in the range of 290–490 nm upon excitation at 280 nm for BSA. Synchronous fluorescence spectra of BSA titrated with various concentrations of DAPC were recorded from 250 to 420 nm ($\Delta\lambda$ = 60 nm) and from 270 to 380 nm ($\Delta\lambda$ = 15 nm) with the excitation and emission slit widths of 2.5 and 2.5 nm, respectively.

The absorption spectra of DAPC (1.0 μmol·L^{-1}) were recorded in the range of 290–490 nm. Then, the overlap of the absorption spectra of DAPC with the fluorescence emission spectrum of BSA was used to calculate the energy transfer. The BSA concentration was fixed at 1.0 μmol·L^{-1}, the UV–Vis absorption spectra and CD spectra of the solution were measured with gradually increasing the concentration of DAPC.

3 Results and Discussion

3.1 The Effect of DAPC on the Fluorescence Emission of BSA

The intrinsic fluorescence of BSA is mainly contributed by the tryptophan residues [23, 24]. Figure 1 shows the effect of DAPC on the fluorescence emission of BSA. It can be observed that BSA had a strong fluorescence emission band at 358 nm when the excited wavelength was selected at 280 nm and DAPC had no intrinsic fluorescence (Fig. 1).

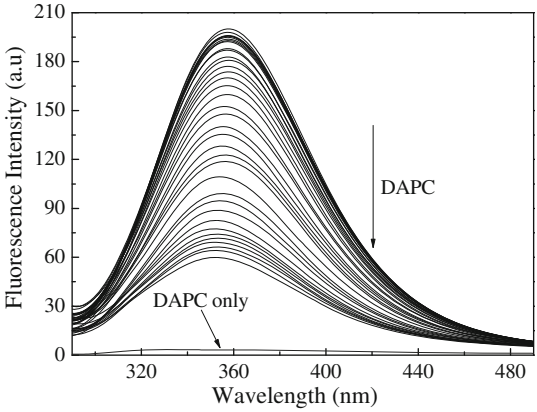

Fig. 1 Fluorescence spectra of BSA with different concentrations of DAPC; *curve m* (*blue line*) shows the fluorescence spectrum of DAPC only (C_{BSA} = 1 μmol·L^{-1}, C_{DAPC} = 5 μmol·L^{-1}, λ_{ex} = 280 nm, pH = 7.4, T = 298 K)

Moreover, with increasing concentration of DAPC, the fluorescence intensity of BSA was quenched by nearly 75 % and a blue shift of 7 nm of the maximum emission wavelength from 358 to 351 nm was observed, indicating that a DAPC–BSA complex was formed.

Amphiphilic molecules with hydrophobic and hydrophilic groups may bind selectively to proteins by hydrophobic/hydrophilic interfaces, because water-soluble globular proteins have hydrophobic functional groups in the interior and hydrophilic groups on the exterior [25]. According to Burstein [26], the maximum emission wavelength of tryptophan residues is extremely sensitive to its environment, and the maximum fluorescence emission wavelength will be 350–353 nm if they are in the aqueous phase; and a blue shift will appear if the protein is exposed to a hydrophobic environment. As shown in Fig. 1, a blue shift of the maximum emission wavelength of BSA from 358 to 351 nm was observed. This indicates that the tryptophan residues of BSA may pass from the aqueous phase into a hydrophobic environment with increases of the DAPC concentration; thus the DAPC may bind selectively at hydrophobic interfaces of BSA.

Fluorescence quenching is usually classified as dynamic quenching or static quenching. In order to obtain the quenching mechanism, the procedure was firstly assumed to be dynamic quenching. For the dynamic quenching, the fluorescence data were then analyzed according to the Stern–Volmer equation [27].

$$\frac{F_0}{F} = 1 + k_q \tau_0 [Q] = 1 + K_{SV}[Q] \quad (1)$$

In Eq. 1, F_0 and F denote the fluorescence intensity in the absence and presence of quencher, respectively, and K_{sv} and k_q represent the Stern–Volmer quenching constant and the bimolecular quenching rate constant, respectively. [Q] is the concentration of the quencher, the average fluorescence lifetime of the macromolecule τ_0 is 10^{-8} s^{-1} for BSA [28]. According to the Stern–Volmer equation and the experimental data, the K_{SV} and k_q were calculated and are listed in Table 1.

Figure 2 shows the Stern–Volmer plots, with good linearity, for the interaction of DAPC with BSA at different temperatures. A small deviation of the Stern–Volmer plots from linearity was observed toward the *y*-axis at higher concentrations of DAPC, indicating that the quenching mechanism of the interaction between DAPC and BSA may be mainly controlled by static quenching according to the reports by Wei et al. [29] and Li et al. [30].

It can be seen from Table 1 that the rate constants ($k_q \times 10^{13}$ $L \cdot mol^{-1} \cdot s^{-1}$) between DAPC and BSA at different temperature are 4.79 (298 K, R = 0.9965), 4.10 (308 K, R = 0.9957) and 3.31 (318 K, R = 0.9933), respectively. All of them are far greater than 2.0×10^{10} $L \cdot mol^{-1} \cdot s^{-1}$. Also, K_{SV} ($\times 10^5$ $L \cdot mol^{-1}$) decreased from 4.79, 4.10 to 3.31 with increasing temperature. In general, the maximum collision-quenching constant of various quenchers with the biopolymer is 2.0×10^{10} $L \cdot mol^{-1} \cdot s^{-1}$ and K_{SV} increases

Table 1 Quenching constants of DAPC with BSA at different temperatures

System	*T*/K	$K_{sv}/10^5$ $L \cdot mol^{-1}$	$K_q/10^{13}$ $L \cdot mol^{-1} \cdot s^{-1}$	R^2
DAPC–BSA	298	4.79	4.79	0.9965
	308	4.10	4.10	0.9957
	318	3.31	3.31	0.9933

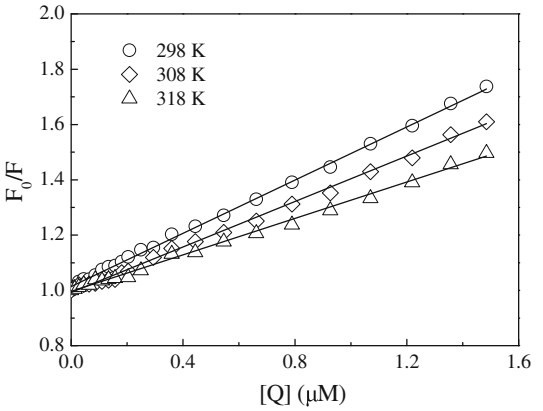

Fig. 2 Stem–Volmer plots for the interaction of DAPC with BSA at different temperatures

with increasing temperature for a dynamic quenching process [31]. Therefore, the quenching mechanism of BSA interacting with DAPC is probably static rather than dynamic quenching, and originates from the formation of a complex between DAPC and BSA.

In order to further prove that it was static quenching, the fluorescence data were further analyzed using the Lineweaver–Burk equation [32]:

$$\frac{F_0}{F_0 - F} = \frac{1}{fK_{\mathrm{LB}}[\mathrm{Q}]} + \frac{1}{f} \tag{2}$$

in which K_{LB} is the static quenching constant and F_0 and F are the same as above. The double-reciprocal plot of $F_0\ (F_0 - F)^{-1}$ versus $[\mathrm{Q}]^{-1}$ is shown in Fig. 3 and K_{LB} calculated from the slope are listed in Table 2.

Table 2 shows that the quenching constant (K_{LB}) decreases with increasing temperature. According to the literature [33], the quenching constant (K_{LB}) increases with the increasing temperature due to the increased collision rate of molecules in the dynamic quenching process. So, the static quenching mechanism is further verified.

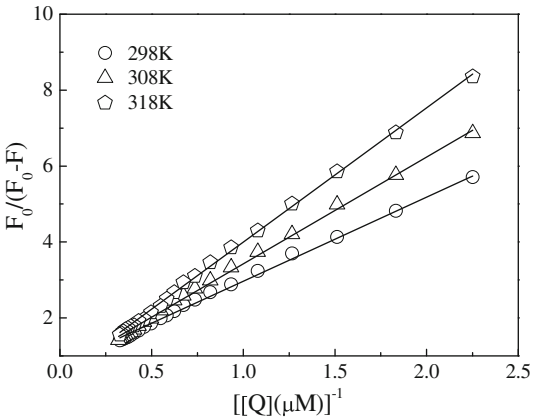

Fig. 3 Plot of the Lineweaver–Burk equation showing the binding of BSA with DAPC at different temperatures

For the static quenching process, the binding constant (K_A) and the number of binding sites (n) can be calculated, as small molecules bind independently to a set of equivalent sites, on a macromolecule by using the following equation [34]:

$$\log_{10}\left[\frac{F_0 - F}{F}\right] = \log_{10} K_A - n \log_{10}[Q] \tag{3}$$

where K_A and n are the binding constant and the number of binding sites, respectively, and [Q] represents the total concentration of quencher. Figure 4 shows the plots of $\log_{10}[(F_0 - F)^{-1}/F]$ against $\log_{10}$ [Q], and the values of K_A and n were obtained from the slopes and intercepts of these plots and are listed in Table 2.

From the data in Table 2, it is clear that there is a strong binding force between DAPC and BSA; the greater the K_A value, the more stable the complex. The decrease of binding constant with increasing temperature indicates a decline in the stability of the DAPC binding to BSA complex. The value of n, which represents the number of binding sites, is close to two, indicating that two binding sites in BSA are accessible to DAPC. Also, n decreases with increasing temperature, suggesting desorption of DAPC or the decomposition of the BSA–DAPC complex.

3.2 Thermodynamic Parameters of the Binding Process

The interactions between a small molecule and a biological macromolecule are noncovalent and include hydrogen bonding, hydrophobic force, electrostatic interaction, and the van der Waals force. The standard enthalpy change (ΔH^0), entropy change (ΔS^0) and Gibbs energy change (ΔG^0) can be used to characterize the binding process. The thermodynamic parameters were calculated by the van't Hoff relations [35]:

$$\ln K = -\frac{\Delta H^0}{RT} + \frac{\Delta S^0}{R} \tag{4}$$

$$\Delta G^0 = -RT \ln K = \Delta H^0 - T\Delta S^0 \tag{5}$$

the plot of ln K versus $1/T$ (Fig. 5) enables the determination of ΔH^0, ΔS^0 and ΔG^0, and these values are presented in Table 3.

As shown in Table 3, ΔH^0 is small and negative, having a value of -15.0 kJ·mol^{-1}, whereas ΔS^0 has a positive value of 57.0 J·mol^{-1}·K^{-1}. The negative enthalpy changes (ΔH^0) and positive entropy changes (ΔS^0) indicate that the binding processes of DAPC to BSA is entropically driven and exothermic. Ross and Subramanian [36] characterized the sign and magnitude of the thermodynamic parameters associated with various individual kinds of interaction that may take place in protein association process. From the water structure viewpoint, a positive ΔS^0 value is generally thought of as an evidence for a

Table 2 The binding constants and the number of binging sites for BSA by DAPC at different temperatures

System	T/K	$K_A/10^5$ L·mol^{-1}	n	$K_{LB}/10^5$ L·mol^{-1}
DAPC–BSA	298 K	4.03	1.69	3.19
	308 K	3.27	1.65	2.03
	318 K	2.78	1.63	1.17

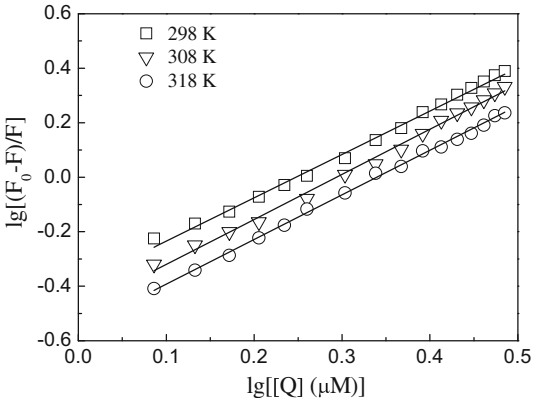

Fig. 4 Double-logarithm relation of $\log_{10}[(F_0 - F)/F]$ versus $\log_{10}[Q]$

hydrophobic interaction because the water molecules that are arranged in an orderly fashion around the DAPC and protein acquire a more random configuration [37]. The negative value of ΔH^0 of -15.0 kJ·mol^{-1} observed in this experiment cannot be attributed mainly to electrostatic interactions, since the value of ΔH^0 is relatively small [13, 36]. Whenever there is a hydrogen bond in the binding reaction, a negative ΔH^0 value will be obtained [36]. Therefore, it is not possible to account for the thermodynamic parameters of the DAPC to BSA complex on the basis of a single intermolecular force. Meanwhile, for the DAPC–BSA system, it is found that the main contribution to ΔG^0 arises from the ΔS^0 term rather than from ΔH^0. So hydrophobic interactions most likely play a major role in the binding of DAPC to BSA, but hydrogen bonding cannot be excluded [36].

3.3 Energy Transfer Between DAPC and BSA

The overlap of the UV–Vis absorption spectrum of DAPC with the fluorescence emission spectrum of BSA is shown in Fig. 6. It is apparent that the fluorescence spectrum of BSA significantly overlaps with the UV–Vis spectrum of DAPC. According to Förster's non-radiative energy transfer theory [38], energy transfer takes place if the distance between BSA and DAPC is smaller than 8 nm. It is well known that the distance between BSA and

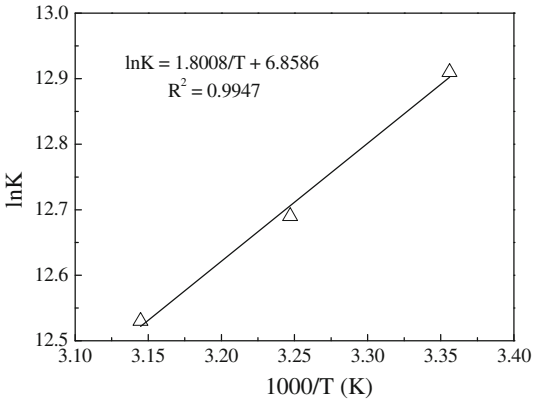

Fig. 5 Van't Hoff plot for the interaction of BSA and DAPC at pH = 7.40

Table 3 The thermodynamic parameters of the interaction of BSA with DAPC

System	T/K	ΔH^0/kJ·mol^{-1}	ΔS^0/J·K·mol^{-1}	ΔG^0/kJ·mol^{-1}
DAPC–BSA	298			−31.98
	308	−14.97	57.02	−32.49
	318			−33.13

DAPC can be calculated according to the Förster's non-radiative energy transfer theory; the energy transfer efficiency (E) is not only related to the distance (r) but also to the critical energy transfer distance (R_0) [39]:

$$E = 1 - \frac{F}{F_0} = \frac{R_0^6}{R_0^6 + r^6} \tag{6}$$

where r and R_0 represent the distance between acceptor and donor, and the critical distance at which the energy transfer efficiency is 50 %, respectively. The value of R_0 calculated using Eq. 7 is:

$$R_0^6 = 8.8 \times 10^{-25} k^2 \bar{n}^{-4} \varphi_0 J \tag{7}$$

where k^2 is the spatial orientation factor that depends on the alignment of the donor and acceptor dipoles, $\bar{n}$ is the refractive index and φ_0 is the luminescence quantum yield. J is the overlap between the emission spectrum of the donor and the absorption spectra of the acceptor, and J is given by:

$$J = \frac{\sum F(\lambda)\varepsilon_A(\lambda)\lambda^4 \Delta\lambda}{\sum F(\lambda)\lambda^4 \Delta\lambda} \tag{8}$$

in which $F(\lambda)$ is the fluorescence intensity of the fluorescent donor in the wavelength λ to $\lambda+\Delta\lambda$ and ε_A is the extinction coefficient of the acceptor at wavelength λ.

According to literature [40], $k^2 = 2/3$, $\varphi_0 = 0.15$ and $\bar{n} = 1.336$ for BSA, and the results calculated using Eqs. 6–8 are listed in Table 4.

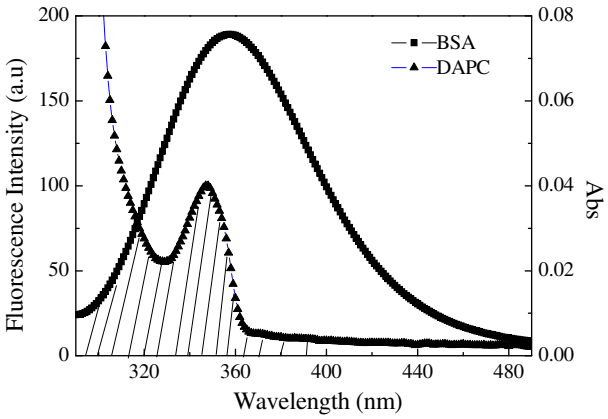

Fig. 6 Overlap of the UV absorption of DAPC with the fluorescence emission spectrum of BSA ($C_{DAPC} = 5.0$ μmol·L^{-1}, $C_{BSA} = 1.0$ μmol·L^{-1} and $T = 298$ K)

Figure 6 shows the large overlap of emission spectra of the donor BSA and the UV–Vis spectra of the acceptor of DAPC. The data in Table 4 show clearly that R_0 and r diminish gradually with the increase of DAPC concentration and both are less than 8 nm; meanwhile the energy transfer efficiency increases, indicating that BSA and DAPC get closer as the concentration increases. All the results indicate that the energy transfer from BSA to DAPC has a high probability.

3.4 Synchronous Fluorescence Spectroscopy Studies

Synchronous fluorescence spectroscopy provides information on the microenvironment of chromophores in BSA. As we know, BSA emits fluorescence due to the presence of Tyr and Trp residues. Thus, synchronous fluorescence spectra of BSA will provide information about the Trp residues or Tyr residues when the wavelength interval ($\Delta\lambda$) are 60 or 15 nm, respectively [41]. Figure 7 shows the fluorescence spectra of BSA with different concentrations of DAPC. With the addition of DAPC, a slight blue shift from 292 to 290 nm of the maximum emission wavelength of Trp residues ($\Delta\lambda = 60$ nm) appeared, the maximum emission wavelength of Tyr residues at $\Delta\lambda = 15$ nm did not have a large shift (from 298 to 297 nm) indicating that the interaction of DAPC with BSA does not affect the microenvironment around Tyr residues, while the Trp residues are placed in a more hydrophobic environment [37, 42]. There is a large hydrophobic cavity in subdomain IIA where both Trp-212 and Tyr-263 residues are located, in which many substances may bind [43]. Therefore, the observation implies that the DAPC molecule may combine with Trp-212 and Tyr-263 of BSA. The shifted emission wavelength for the Trp and Tyr residues suggests that DAPC has changed the conformation of BSA.

Figure 7 shows that the synchronous fluorescence intensities of Trp residues on BSA decreased by 66.95 % at various concentrations of DAPC. The fluorescence quenching of Tyr residues on BSA decreased by 46.28 % in the presence of DAPC. Thus, the fluorescence quenching of Trp residues is much larger than that of Tyr residues, which indicates that Trp residues contributed more to the quenching of intrinsic fluorescence and DAPC is more accessible to the Trp residues on BSA.

3.5 UV–Vis Absorption Spectroscopy

UV–Vis absorption can be applied to detect the structural changes of protein and understand the complex formation process [44]. Therefore, the effect of various amounts of DAPC on the structural changes of BSA was studied by UV–Vis spectra. As shown in Fig. 8, upon addition of DAPC to BSA, the UV absorbance intensity of BSA at 280 nm increased. It shows that the DAPC–BSA complex formed and the conformation of BSA changed [45]. Moreover, it further confirms the quenching of BSA by DAPC is static

Table 4 Parameters of energy transfer between BSA (1.0 μmol·L^{-1}) and DAPC of different concentration

C_{DAPC}/μmol·L^{-1}	J/10^{-15} cm^3·L·mol^{-1}	E	R_0/nm	R/nm
1.00	11.52	0.35	2.61	2.90
2.00	4.49	0.54	2.23	2.17
3.00	2.88	0.70	2.07	1.80

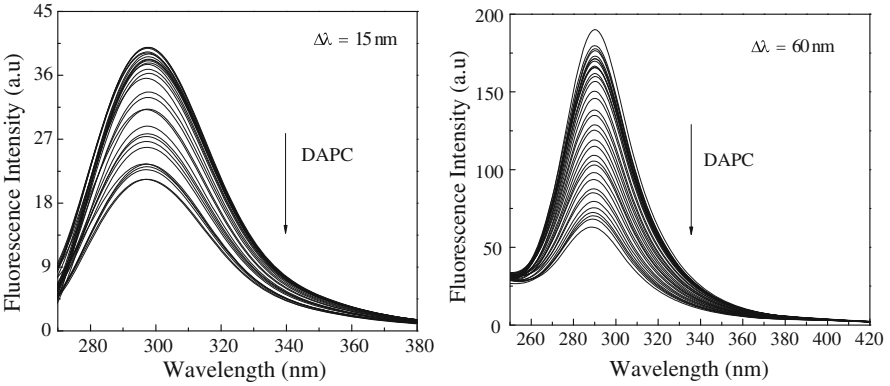

Fig. 7 Synchronous fluorescence spectra of the DAPC–BSA complex (C_{BSA} = 1.0 μmol·L^{-1}, C_{DAPC} = 5 μmol·L^{-1}, T = 298 K and pH = 7.40)

quenching, i.e., the fluorescence quenching of BSA arising from the DAPC–BSA complex is predominant, while that from dynamic collision could be negligible [46]. Meanwhile, a moderate blue shift ($\Delta\lambda$ = 2–3 nm) of the maximum absorption wavelength appeared upon addition of DAPC to BSA. This phenomenon indicates the conformation of BSA changed, the polarity around the tryptophan residues increased and the hydrophobicity decreased [40]. This conclusion agrees with the other results of conformational changes by UV–Vis spectra [47].

3.6 Circular Dichroism

CD spectroscopy is a quantitative technique to monitor the conformational changes of protein upon interaction with small molecules. Figure 9 shows CD spectra of BSA with different concentrations of DAPC. It is obvious that the pure BSA exhibites two strong double minimum signals at 220 and 208 nm, which correspond to the characteristic signals of the α-helix structure of BSA [48]. With the addition of DAPC to BSA, the intensity of

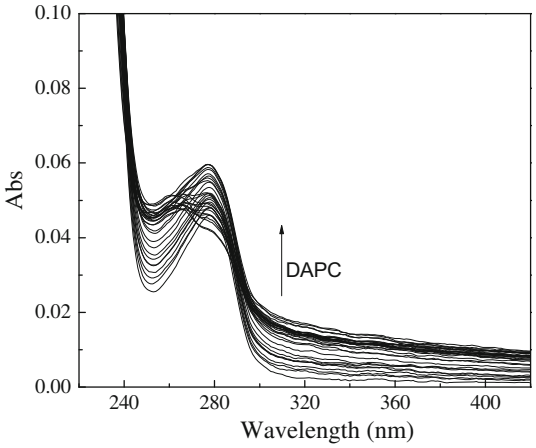

Fig. 8 UV–Vis absorption spectra of BSA in various concentrations of DAPC. (C_{BSA} = 1 μmol·L^{-1}, C_{DAPC} = 5 μmol·L^{-1}, T = 298 K and pH = 7.40)

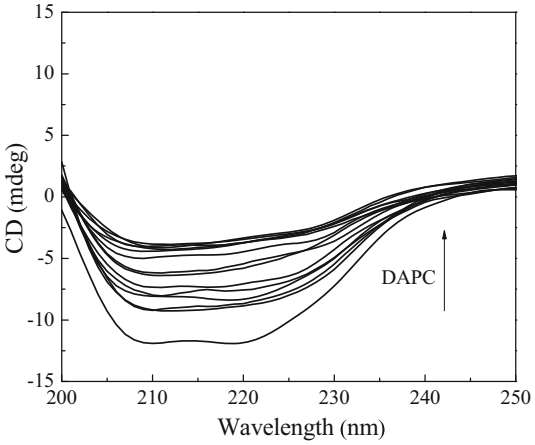

Fig. 9 CD spectra of DAPC interacting with BSA ($C_{BSA} = 1$ μmol·L^{-1}, $C_{DAPC} = 5$ μmol·L^{-1}, $T = 298$ K and pH = 7.40)

the double minimum signals of α-helicity of BSA decreased, indicating that the α-helix content decreased when DAPC is bound to BSA [49]. The results can be expressed in terms of the mean residue ellipticity (MRE) in deg·cm^2·dmol^{-1}, according to the following Eq. 9 [50]

$$[\theta] = \frac{\theta_{obs}}{10nlC_p} \tag{9}$$

where θ_{obs} is the CD in millidegrees, n the number of amino acid residues (583), l the path length of the cell (0.1 cm), and C_p is the mole fraction. The α-helical content can be calculated from the $[\theta]$ values at 208 nm using the following Eq. 10 [51]:

$$\alpha - \text{helix } (\%) = \frac{-[\theta]_{208} - 4,000}{33,000 - 4,000} \tag{10}$$

According to the above equations, the percentage α-helix content of BSA was calculated. The results indicate that the α-helix content of BSA changed from that of 55.0 % for free BSA to 38.3 % for the BSA–DAPC system. The decreasing α-helix content suggests that the binding of DAPC with BSA induces a slight unfolding of the constituent polypeptides of the protein, some secondary-structure changes in BSA, and the exposure of some hydrophobic regions (which were earlier buried) increased. This is consistent with the results of the synchronous fluorescence.

4 Conclusions

In this work, the interaction between DAPC and BSA was investigated by different spectroscopic techniques including fluorescence spectroscopy, UV–Vis absorption spectroscopy and circular dichroism spectroscopy. The results show that the fluorescence quenching of BSA is initiated by DAPC and the quenching mechanism is static quenching. In the binding of DAPC and BSA the hydrophobic interaction plays a major role. The average binding distance between the donor (BSA) and the acceptor (DAPC) is less than

8 nm. Furthermore, the secondary structure of BSA molecules is changed in the presence of DAPC.

Acknowledgments This work was supported by the Science Research Project of the Ministry of Education of Heilongjiang Province of China (2012TD012, 12511Z030), the National Natural Science Foundation of Heilongjiang Province (B201114, B201313) and the Science Research Project of Key Laboratory of Fine Chemicals of College of Heilongjiang Province of China (JX201210).

References

1. Dudev, T., Lim, C.: Principles governing Mg, Ca, and Zn binding and selectivity in proteins. Chem. Rev. **103**, 773–788 (2003)
2. Ruso, J.M., Deo, N., Somasundaran, P.: Complexation between dodecyl sulfate surfactant and zein protein in solution. Langmuir **20**, 8988–8991 (2004)
3. Liu, J.Q., Tian, J.N., Tian, X., Hu, Z.D.: Interaction of isofraxidin with human serum albumin. Bioorg. Med. Chem. **12**, 469–474 (2004)
4. Zhang, L.N., Wu, F.Y., Liu, A.H.: Study of the interaction between 2,5-di-[2-(4-hydroxy-phenyl) ethylene]-terephthalonitril and bovine serum albumin by fluorescence spectroscopy. Spectrochim. Acta A **79**, 97–103 (2011)
5. He, W.Y., Li, Y., Hu, Z.: Specific interaction of chalcone–protein: cardamonin binding site II on the human serum albumin molecule. Biopolymers **79**, 48–57 (2005)
6. Liu, Y.H., Zhang, L.J., Liu, R.T.: Spectroscopic identification of interactions of Pb^{2+} with bovine serum albumin. J. Fluoresc. **22**, 239–245 (2012)
7. Yang, Y., Yu, X., Tong, W., Lu, S., Liu, H., Yao, Q., Zhou, H.: Investigation of the interaction between novel spiro thiazolo [3,2-a][1,3,5] triazines and bovine serum albumin by spectroscopic methods. J. Solution Chem. **42**, 666–675 (2013)
8. Zhou, T., Ao, M.Q., Xu, G.Y., Liu, T.: Interactions of bovine serum albumin with cationic imidazolium and quaternary ammonium gemini surfactants: Effects of surfactant architecture. J. Colloid Interface Sci. **389**, 175–181 (2013)
9. Zhao, R., Xie, Y., Tan, Y., Tan, C., Jiang, Y.: Binding of a bcl-2 family inhibitor to bovine serum albumin: fluorescence quenching and molecular docking study. Protein Pept. Lett. **19**, 945–954 (2012)
10. Fainerman, V.B., Zholob, S.A., Leser, M.: Competitive absorption from mixed nonionic surfactant/protein solutions. J. Colloid Interface Sci. **274**, 496–501 (2004)
11. Yao, Q., Yu, X., Zheng, T., Liu, H., Yang, Y., Yi, P.: Spectroscopic studies on the interaction of carteolol hydrochloride and urea-induced bovine serum albumin. Spectrochim. Acta A **113**, 447–451 (2013)
12. Turro, N.J., Lei, X.G., Ananthapadmanabhan, K.P., Aronson, M.: Spectroscopic probe analysis of protein–surfactant interactions: the BSA/SDS system. Langmuir **11**, 2525–2533 (1995)
13. Duan, L., Yang, L., Xiong, H., Zhang, X., Wang, S.: Studies on the electrochemistry of rutin and its interaction with bovine serum albumin using a glassy carbon electrode modified with carbon-coated nickel nanoparticles. Microchim. Acta **180**, 355–361 (2013)
14. Sharma, A., Pasha, J.M., Deep, S.: Effect of the sugar and polyol additives on the aggregation kinetics of BSA in the presence of N-cetyl-N, N, N-trimethyl ammonium bromide. J. Colloid Interface Sci. **350**, 240–248 (2010)
15. Usman, M., Siddiq, M.: Surface and micellar properties of chloroquine diphosphate and its interactions with surfactants and human serum albumin. J. Chem. Thermodyn. **58**, 359–366 (2013)
16. Lissi, E., Abuin, E., Lanio, M.E.: A new and simple procedure for the evaluation of the association of surfactants to proteins. J. Biochem. Biophys. Methods **50**, 261–268 (2002)
17. Gelamo, E.L., Silva, C.H.T.P., Imasato, H., Tabak, M.: Interaction of bovine (BSA) and human (HSA) serum albumins with ionic surfactants: spectroscopy and modelling. Biochim. Biophys. Acta **1594**, 84–99 (2002)
18. Mote, U.S., Han, S.H., Patil, S.R., Kolekar, G.B.: Effect of temperature and pH on interaction between bovine serum albumin and cetylpyridinium bromide: fluorescence spectroscopic approach. J. Lumin. **130**, 2059–2064 (2010)
19. Quagliotto, P., Barbero, N., Barolo, C., Artuso, E.: Synthesis and properties of cationic surfactants with tuned hydrophylicity. J. Colloid Interface Sci. **340**, 269–275 (2009)

20. Buciñski, A., Socha, A., Wnuk, M., Bqczek, T., Nowaczyk, A.: Artificial neural networks in prediction of antifungal activity of a series of pyridine derivatives against Candida albicans. J. Microbiol. Methods **76**, 25–29 (2009)
21. Loftsson, T., Thorsteinsson, T., Másson, M.: Hydrolysis kinetics and QSAR investigation of soft antimicrobial agents. J. Pharm. Pharmacol. **57**, 721–727 (2005)
22. Sundararaman, M., Kumar, R.R., Venkatesan, P., llangovan, A.: 1-Alkyl-(N,N-dimethy lamino)pyridinium bromides: inhibitory effect on virulence factors of Candida albicans and on the growth of bacterial pathogens. J. Med. Microbiol. **62**, 241–248 (2013)
23. Wang, Q., Yan, J., He, J., Bai, K., Li, H.: Characterization of the interaction between 3-oxotabersonine and two serum albumins by using spectroscopic techniques. J. Lumin. **138**, 1–7 (2013)
24. Abou-Zied, O.K., Al-Shihi, O.I.: Characterization of subdomain IIA binding site of human serum albumin in its native, unfolded, and refolded states using small molecular probes. J. Am. Chem. Soc. **32**, 10793–10801 (2008)
25. Wu, D., Wei, Q., Du, Y.: Quenching of the intrinsic fluorescence of bovine serum albumin by phenylfluorone–Mo(VI) complex as a probe. Int. J. Biol. Macromol. **37**, 69–72 (2005)
26. Burstein, E.A., Vedenkina, N.S., Ivkova, M.N.: Fluorescence and the location of tryptophan residues in protein molecules. Photochem. Photobiol. **18**, 263–279 (1973)
27. Paramaguru, G., Kathiravan, A., Selvaraj, S., Venuvanalingam, P.: Interaction of anthraquinone dyes with lysozyme: evidences from spectroscopic and docking studies. J. Hazard. Mater. **175**, 985–991 (2010)
28. Gong, A.Q., Zhu, X.S., Hu, Y.Y., Yu, S.H.: A fluorescence spectroscopic study of the interaction between epristeride and bovin serum albumin and its analytical application. Talanta **73**, 668–673 (2007)
29. Wei, Y.L., Li, J.Q., Dong, C., Shuang, S.M., Liu, D.S.: Investigation of the association behaviors between biliverdin and bovine serum albumin by fluorescence spectroscopy. Talanta **70**, 377–382 (2006)
30. Li, L., Wang, Y., Song, G., Wu, S., Chu, P.K., Xu, Z.: Bonding strength of fluorinated and hydrogenated surfactant to bovine serum albumin. J. Fluorine Chem. **130**, 870–877 (2009)
31. Tu, S., Jiang, X., Zhou, L., Yin, W., Wang, H., Duan, M., Liu, P., Jiang, X.: Study of the interaction of gemini surfactant NAE12-4-12 with bovine serum albumin. J. Lumin. **132**, 381–385 (2012)
32. Ashoka, S., Seetharamappa, J., Kandagal, P.B., Shaikh, S.M.T.: Investigation of the interaction between trazodone hydrochloride and bovine serum albumin. J. Lumin. **121**, 179–186 (2006)
33. Wang, H., Jiang, X., Zhou, L., Cheng, Z., Yin, W., Duan, M., Liu, P., Jiang, X.: Interaction of NAEn-s-n gemini surfactants with bovine serum albumin: a structure-activity probe. J. Lumin. **134**, 138–147 (2013)
34. Cheng, Z.J., Zhang, Y.T.: Spectroscopic investigation on interaction of the bioactive component dl-tetrahydropalmatine to bovine serum albumin. J. Mol. Struct. **876**, 308–312 (2008)
35. Sarkar, M., Paul, S.S., Mukherjea, K.K.: Interaction of bovine serum albumin with a psychotropic drug alprazolam: physicochemical, photophysical and molecular docking studies. J. Lumin. **142**, 220–230 (2013)
36. Ross, P.D., Subramanian, S.: Thermodynamics of protein association reactions: forces contributing to stability. Biochemistry **20**, 3096–3102 (1981)
37. Cheng, Z.J.: Interaction of ergosterol with bovine serum albumin and human serum albumin by spectroscopic analysis. Mol. Biol. Rep. **39**, 9493–9508 (2012)
38. Cristobel, G., Dos, R., Pierre, D.J.M.: Fluorescence resonance energy transfer spectroscopy reliable "ruler" for measuring structural changes in proteins. J. Struct. Biol. **115**, 175–185 (1995)
39. Qin, Y., Zhang, Y., Yan, S., Ye, L.: A comparison study on the interaction of hyperoside and bovine serum albumin with Tachiya model and Stern–Volmer equation. Spectrochim. Acta A **75**, 1506–1510 (2010)
40. Kumar, R.S., van den Bergh, H., Wagnières, G.: Probing the interaction between a surfactant–cobalt (III) complex and bovine serum albumin. J. Solution Chem. **41**, 294–306 (2012)
41. Guo, X.J., Hao, A.J., Han, X.W., Kang, P.L., Jiang, Y.C., Zhang, X.J.: The investigation of the interaction between ribavirin and bovine serum albumin by spectroscopic methods. Mol. Biol. Rep. **38**, 4185–4192 (2011)
42. Yu, X., Liu, R., Yang, F., Ji, D., Li, X., Chen, J., Huang, H., Yi, P.: Study on the interaction between dihydromyricetin and bovine serum albumin by spectroscopic techniques. J. Mol. Struct. **985**, 407–412 (2011)
43. Wang, C.X., Yan, F.F., Zhang, Y.X., Ye, L.: Spectroscopic investigation of the interaction between rifabutin and bovine serum albumin. J. Photochem. Photobiol. A **192**, 23–28 (2007)
44. Chen, J., Jiang, X.Y., Chen, X.Q., Chen, Y.: Effect of temperature on the metronidazole–BSA interaction: multi–spectroscopic method. J. Mol. Struct. **876**, 121–126 (2008)

45. Kandagal, P.B., Seetharamappa, J., Shaikh, S.M.T., Manjunatha, D.H.: Binding of trazodone hydrochloride with human serum albumin: a spectroscopic study. J. Photochem. Photobiol. A **185**, 239–244 (2007)
46. Zhu, G.F., Wang, Y., Liu, J., Wang, H., Xi, L., Du, L.F.: Interaction between ginkgolic acid and human serum albumin by spectroscopy and molecular modeling methods. J. Solution Chem. **43**, 1232–1249 (2014)
47. Li, J.F., Li, J.Z., Jiao, Y., Dong, C.: Spectroscopic analysis and molecular modeling on the interaction of jatrorrhizine with human serum albumin (HSA). Spectrochim. Acta A **118**, 48–54 (2014)
48. Shahabadi, N., Maghsudi, M.: Binding studies of a new copper(II) complex containing mixed aliphatic and aromatic dinitrogen ligands with bovine serum albumin using different instrumental methods. J. Mol. Struct. **929**, 193–199 (2009)
49. Hu, Y.J., Liu, Y., Shen, X.S., Fang, X.Y., Qu, S.S.: Studies on the interaction between 1-hexylcarbamoyl-5-fluorouracil and bovine serum albumin. J. Mol. Struct. **738**, 143–147 (2005)
50. Mandal, G., Bardhan, M., Ganguly, T.: Interaction of bovine serum albumin and albumin–gold nanoconjugates with l-aspartic acid. a spectroscopic approach. Colloids Surf. B **81**, 178–184 (2010)
51. Hu, Y.J., Yue, H.L., Li, X.L., Zhang, S.S.: Molecular spectroscopic studies on the interaction of morin with bovine serum albumin. J. Photochem. Photobiol. B **112**, 16–22 (2012)